

Supporting Information

Moore et al. 10.1073/pnas.1312933110

SI Experimental Procedures

Animals. Using the same genomic clone that was used for generating the *Trpv4*^{-/-} pan-null mouse (1), the *Trpv4* targeting construct was electroporated into mouse ES cells (C57BL6 background), and orthotopic integration was verified by PCR and Southern blot. The engineered mutation was introduced into the germ line by mating of chimeric mice with C57BL6 WT mice. The selection marker was deleted by FLPe-mediated excision of the frt-pGK-neo-frt cassette in FLPe deleter mice (2). Genotyping was accomplished by PCR and PaeI digest; primer sequences are available on request and as in ref. 1 (Fig. S1B).

Chemicals/Biologicals. We used the following biologicals and compounds: endothelin-1 (ET1); BQ123 and BQ788 [endothelin receptor, ET(R), blockers for ET(R)-A and ET(R)-B] (Sigma); U73122 [phospholipase C (PLC) inhibitor] (Tocris); 4 α -phorbol 12,13 didecanoate (4 α -PDD, TRPV4 activator) (Tocris); GSK205 (TRPV4 inhibitor) (3–5); RN-1734 (TRPV4 inhibitor) (Tocris); CGS35066 (endothelin-converting enzyme inhibitor) (Tocris); isopentenyl pyrophosphate (IPP, TRPV3 inhibitor) (Sigma); and camphor (TRPV3 activator) (Whole Foods).

Behavioral Assessment of Withdrawal Thresholds and Nocifensive Behavior. Behavioral tests were performed to evaluate the decrease in withdrawal thresholds in response to mechanical or thermal stimuli applied to hind paws. These withdrawal thresholds were ascertained before and after UVB exposure. Mice were confined by Plexiglas enclosures on top of a 25- × 26-cm Bio-Rad Gel Doc 2000 UV transilluminator (302 nm), and otherwise allowed to openly explore this environment. UV exposure lasted for 5 min with an exposure of 600 mJ/cm² (6), equivalent to 5–10 minimal erythema-inducing dose (MED). Thorough observations upon initiation of this method demonstrated that hind paws were exposed to UV throughout this period and that animals did not engage in licking behavior during UVB exposure.

Automated von Frey Hair Testing. Hind-paw mechanical withdrawal thresholds were determined by the automated von Frey hair method, as described previously (1, 7), using a 0.5-mm-diameter stainless steel filament, part of an automated plantar touch stimulator (Ugo Basile). Relevant details included pretest acclimatization in a quiet room for 30 min, conducting the test at the same time of day, and blinded observers. The stimulus was delivered to the hind paw, automatically discontinued upon withdrawal, and its intensity recorded automatically. Six to eight trials per animal were conducted, with equal exposure of both hind paws, leading to an average withdrawal threshold. Results are reported as Δ -threshold, which was calculated by subtracting posttreatment from pretreatment measurements, expressed as percent or relative to 1.0.

Hargreaves' Test. Hind-paw thermal (hot) withdrawal thresholds were determined by the well-established Hargreaves' method (1, 8), using an infrared thermal stimulation device that delivers the stimulus from underneath the hind paw combined with automatic shut-off upon withdrawal (Ugo Basile). Stimulation and measurements were conducted as described for von Frey hair testing. A cutoff of 20 s was set to prevent tissue damage.

Formalin-Induced Nocifensive Behavior. Videos were read by blinded observers for the total amount of time each mouse spent flinching or licking the injected hind paw.

Mouse Tissue Processing for 1- μ m Semithin Sections and Electron Microscopy. Samples were fixed in 2% glutaraldehyde, 4% paraformaldehyde (PFA), and 2 mM CaCl₂ in 0.05 M sodium cacodylate buffer, pH 7.2, at room temperature for >1 h, dehydrated, postfixed in 1% osmium tetroxide, and processed for Epon embedding. Semithin sections (1 μ m) were stained with toluidine blue and photographed with an Axioplan 2 microscope (Zeiss). For EM analysis, ultrathin sections (60–70 nm) were counterstained with uranyl acetate and lead citrate. EM images were taken with a transmission electron microscope (Tecnaï G2-12; FEI) equipped with a digital camera (XR60; Advanced Microscopy Techniques).

Mouse Tissue Processing for qRT-PCR. Total RNA was extracted from paw tissue using Trizol. 1 μ g RNA was reverse transcribed using superscript II (Invitrogen). Roche Applied Science Light Cycler System was used to analyze expression. Gene expression was normalized against GAPDH. The $\Delta\Delta$ Ct method was used. IL-6 expression was determined by using primers sense 5'-TG-GTACTCCAGAAGACCAGAGG and antisense 5'-AACGATGATGCACTTGCAGA and ET1 expression by using sense 5'-TTCCCCTGATCCTTCTCTCTGCT and antisense 5'-TC-TGCTTGGCAGAAATTCCA. GAPDH sense 5'-GCCTTC-TCCATGGTGGTAA and antisense 5'-GCACAGTCAAGG-CCGAGAAT.

Mouse Tissue Processing for Immunohistochemistry. Routine procedures were followed as described previously (9). Mice were perfused transcardially with 30 mL PBS, followed by 30 mL 4% PFA. Tissues, including the L5 dorsal root ganglia (DRG) (bilateral) and footpad preparations, were dissected and postfixed in 4% PFA. Tissue blocks were further cryoprotected in 30% sucrose in PBS for 24–48 h. For mouse TRPV4, keratin-specific antibodies, phospho-ERK, and IL-6, tissue was prepared as frozen blocks and subsequently sectioned on a cryostat. For CD68 and CD15 (neutrophil elastase), mouse skin was prepared by 2% PFA perfusion. Footpad was sectioned at 6- μ m and DRG at 10- μ m thickness. Sections were thaw-mounted, blocked with 5% normal goat serum (Jackson), then incubated overnight at 4 °C with the following primary antibodies: rabbit anti-TRPV4 (1:300; Abcam), mouse anti-keratin 14 (1:300, against C-terminal peptide beyond residue 850; Abcam), rabbit anti-keratin 14 (1:1,000; Fuchs Laboratory), rabbit anti-phospho-ERK1/2 (1:500; Cell Signaling Technologies), goat anti-IL-6 (1:200; Santa Cruz Biotechnology Inc.), anti-CD68 and anti-CD15 (AbDSerotec), and rat monoclonal anti-keratin 8 (1:500, TROMA-I antibody; Iowa Developmental Studies Hybridoma Bank). Immunodetection was accomplished with appropriate fluorescently labeled secondary antibodies (AlexaFluor595, AlexaFluor488-conjugated antibodies at 1:600; Invitrogen; for CD15 biotinylated secondary antibody from donkey, 1:400 followed by rhodamine-streptavidin 1:250), or with peroxidase-linked detection reagents (for CD68) for 2 h at room temperature. Sections were rinsed, mounted, and coverslipped with fluoromount (Sigma). Digital micrographs were obtained using a BX61 Olympus upright microscope, also with a Zeiss LSM510 or LSM780 confocal, both equipped with a high-resolution CCD camera, and acquired with constant exposure settings, using ISEE or Zeiss Zen software. Morphometric analysis was conducted using ImageJ software (v1.45) with tailored regions of interest that spared the nuclear compartment. ImageJ was also used for determination of DRG surface area.

Human Tissue Specimens Immune Labeling. Human tissue was deparaffinized with xylene and ethanol series then washed in PBS and incubated at 80 °C for 20 min in Antigen Retrieval buffer (Biogenex). Subsequently, specimens were washed in PBS. Endogenous peroxidase was blocked with 0.3% H₂O₂ + 0.01% sodium azide in PBS for 10 min at room temperature, followed by washing steps in PBS. Blocking was performed in 5% normal horse serum + 0.3% Triton X-100 in PBS for 1 h at room temperature. Primary antibodies [anti-TRPV4 (Abcam) same as for mouse, 1: 8,000; anti-ET1 as for mouse tissue] were incubated overnight at 4 °C in Ventana Antibody dilution buffer (Fisher). After washing in PBS, specimens were incubated with biotinylated donkey-anti-rabbit secondary (BA-1000; Vector) in diluted blocking buffer for 30 min. After washing with PBS, Avidin-Biotin block was applied (PK4000; Vector) for 30 min at room temperature, and the positive immunoreactivity was visualized with 3,3'-diaminobenzidine (DAB) (NC9567138; Fisher). After washing in water, hematoxylin was used to counterstain nuclei. Tissues were washed, dehydrated, and then mounted in Permount (Fisher). For morphometric quantification of TRPV4 and ET1, five sections from each patient and healthy volunteers ($n = 3$ per group) were examined at a magnification of 20 \times and photographed. The entire section was digitalized using Leica software and analyzed using ImageJ. For quantification, DAB and H&E staining in three randomly selected epidermal regions (3.5×1.25 inches) of each image were separated using the IsoData thresholding method in the color threshold plugin. Relative signal intensities were calculated from background-corrected measurements. Values are expressed as mean of averages determined from five sections per patient. Quantification of human skin tissue for TRPV4 and ET1 was performed from acute UV overexposure compared with healthy skin ($n = 3$ per group).

Primary Mouse Keratinocyte Cell Culture. Following protocols based on refs. 10–12, the epidermis was separated from the dermis by a 1-h dispase (BD Biosciences) treatment. Then the keratinocytes were dissociated from the epidermis using trypsin. Keratinocytes were plated on collagen-coated dishes or glass or quartz coverslips and grown in keratinocyte serum-free media (Gibco) supplemented with bovine pituitary extract and EGF (R&D Systems), 100 pmol cholera toxin (Calbiochem), and 1 \times antibiotics/antimycotics (Gibco) in an incubator at 5% CO₂ and 37 °C.

UVB Stimulation of Cultured Keratinocytes and Ca²⁺ Imaging. Ca²⁺ imaging of primary mouse epidermal keratinocytes (1^oMK) in response to chemical activation of TRPV4 was conducted after loading with 2 μ M fura2-AM, following a ratiometric Ca²⁺-imaging protocol with 340/380 nm blue light for dual excitation (5). Ratios of emissions were acquired at 0.5 Hz. $\Delta R/R_0$ was determined as the fraction of the increase of a given ratio over baseline ratio, divided by baseline ratio. For stimulation of cells with UVB, where fura-2 was not suitable because of the proximity of stimulation with 340/380 nm vs. 295 nm, 2 μ M fluo4-AM was used instead. Ca²⁺ imaging was carried out as described (13) at 488 nm excitation, acquisition of emissions at 0.5 Hz, expressed as $\Delta F/F_0$.

In the custom-built UV optical system, UV light-emitting diodes (LEDs) were capped with a ball lens, a transparent optical window in the shape of a hemispherical lens (Fig. S3B). The LED

output optical beam focused at 15~20 mm from the lens, with a spot diameter of approximately 1.5~2.0 mm (Fig. S3C). The electrical power supply for the UV LEDs was a surface-mount component on the printed circuit board, which had a steady-state 20-mA current output that was controlled by an external switch. The thermal equilibration stage was set for physiological temperature. We confirmed the nonthermal nature of UVB stimulation using the customized 295-nm LED device in a dedicated experiment (Fig. S3D), thus confirming the specific modality of stimulation as UVB.

Keratinocyte UV Irradiation Using 295-nm LED and Immunocytochemistry.

Mouse keratinocytes were cultured on collagen-coated quartz coverslips and then stimulated from the bottom using the previously mentioned UV optical system using the 295-nm LED. Twenty-four hours later the cells were fixed in 4% formaldehyde in PBS for 20 min, permeabilized with 0.1% Triton X-100 in PBS for 10 min, washed, then blocked in 10% normal goat serum in PBS for 45 min. Coverslips were incubated overnight with primary antibody mouse anti-ET1 (1:200; Abcam), washed three times in PBS, and incubated with secondary antibody for 2 h at 25 °C. Coverslips were washed three times in PBS, once with double-distilled H₂O. Digital images were captured using a 40 \times immersion lens on the BX61 Olympus upright microscope. Morphometric analysis was conducted using ImageJ software with tailored regions of interest.

Determining UVB Permeation of the Skin. First, the spot size of the UV input optical beam from a LED (UVTOP-295 UV) was estimated, as shown in Fig. S6A, using the razor-edge optical spot occlusion method (results shown in Fig. S6B). The UV LED was powered with 20 mA of current, resulting in 500 μ W of optical power in a circular focal spot 1.5 mm in diameter, with 70% of the total flux in a 0.5-mm beam radius. The UV optical power transmitted through the sample was detected by a Hamamatsu S127-66BR UV detector, and the output of the photodetector was measured using a Keithley 236 source measure unit. GSK205 was administered to the foot-pad skin of live mice in an alcohol and glycerol solution as for the experiments shown in Fig. 7A. The vehicle-control group was treated with the alcohol and glycerol solution only. Another control group consisted of a commercially available SPF100 preparation sunscreen in the form of a cream, which was applied similar to the vehicle control. All applications were made to live mice directly before they were killed and subsequent dissection of foot-pad epidermis. Next, the dissected epidermis was measured for UV transmission by placing it on a quartz coverslip and exposing it to the UV beam. The data for the GSK205 and sunscreen were normalized to this control data.

Western Blotting. Samples were separated by SDS/PAGE and transferred to PVDF membranes (Bio-Rad). Membranes were blocked with dry milk then probed with primary antibodies (rabbit anti-TRPV4, immunogen was final C-terminal epitope of TRPV4 as for immunolabeling; Alomone), mouse anti- β -actin (clone AC-5; Abcam), and mouse anti- β -tubulin (Iowa Hybridoma Bank), followed by horseradish peroxidase-conjugated secondary antibodies (Jackson ImmunoResearch). Secondary antibodies were detected using Supersignal West Dura Extended Duration substrate (Amersham).

1. Liedtke W, Friedman JM (2003) Abnormal osmotic regulation in *trpv4*^{-/-} mice. *Proc Natl Acad Sci USA* 100(23):13698–13703.
2. Dymecki SM (1996) Flp recombinase promotes site-specific DNA recombination in embryonic stem cells and transgenic mice. *Proc Natl Acad Sci USA* 93(12):6191–6196.
3. Vincent F, Dunton MA (2011) TRPV4 agonists and antagonists. *Curr Top Med Chem* 11(17):2216–2226.
4. Phan MN, et al. (2009) Functional characterization of TRPV4 as an osmotically sensitive ion channel in porcine articular chondrocytes. *Arthritis Rheum* 60(10):3028–3037.

5. Li J, et al. (2011) TRPV4-mediated calcium influx into human bronchial epithelia upon exposure to diesel exhaust particles. *Environ Health Perspect* 119(6): 784–793.
6. Bishop T, et al. (2007) Characterisation of ultraviolet-B-induced inflammation as a model of hyperalgesia in the rat. *Pain* 131(1-2):70–82.
7. Balonov K, Khodorova A, Strichartz GR (2006) Tactile allodynia initiated by local subcutaneous endothelin-1 is prolonged by activation of TRPV-1 receptors. *Exp Biol Med (Maywood)* 231(6):1165–1170.

- Hargreaves K, Dubner R, Brown F, Flores C, Joris J (1988) A new and sensitive method for measuring thermal nociception in cutaneous hyperalgesia. *Pain* 32(1):77–88.
- Chen Y, Willcockson HH, Valtchanoff JG (2009) Vanilloid receptor TRPV1-mediated phosphorylation of ERK in murine adjuvant arthritis. *Osteoarthritis Cartilage* 17(2):244–251.
- Wang X, Zinkel S, Polonsky K, Fuchs E (1997) Transgenic studies with a keratin promoter-driven growth hormone transgene: prospects for gene therapy. *Proc Natl Acad Sci USA* 94(1):219–226.
- Vasioukhin V, Bauer C, Degenstein L, Wise B, Fuchs E (2001) Hyperproliferation and defects in epithelial polarity upon conditional ablation of alpha-catenin in skin. *Cell* 104(4):605–617.
- Vasioukhin V, Bowers E, Bauer C, Degenstein L, Fuchs E (2001) Desmoplakin is essential in epidermal sheet formation. *Nat Cell Biol* 3(12):1076–1085.
- Liedtke W, et al. (2000) Vanilloid receptor-related osmotically activated channel (VR-OAC), a candidate vertebrate osmoreceptor. *Cell* 103(3):525–535.

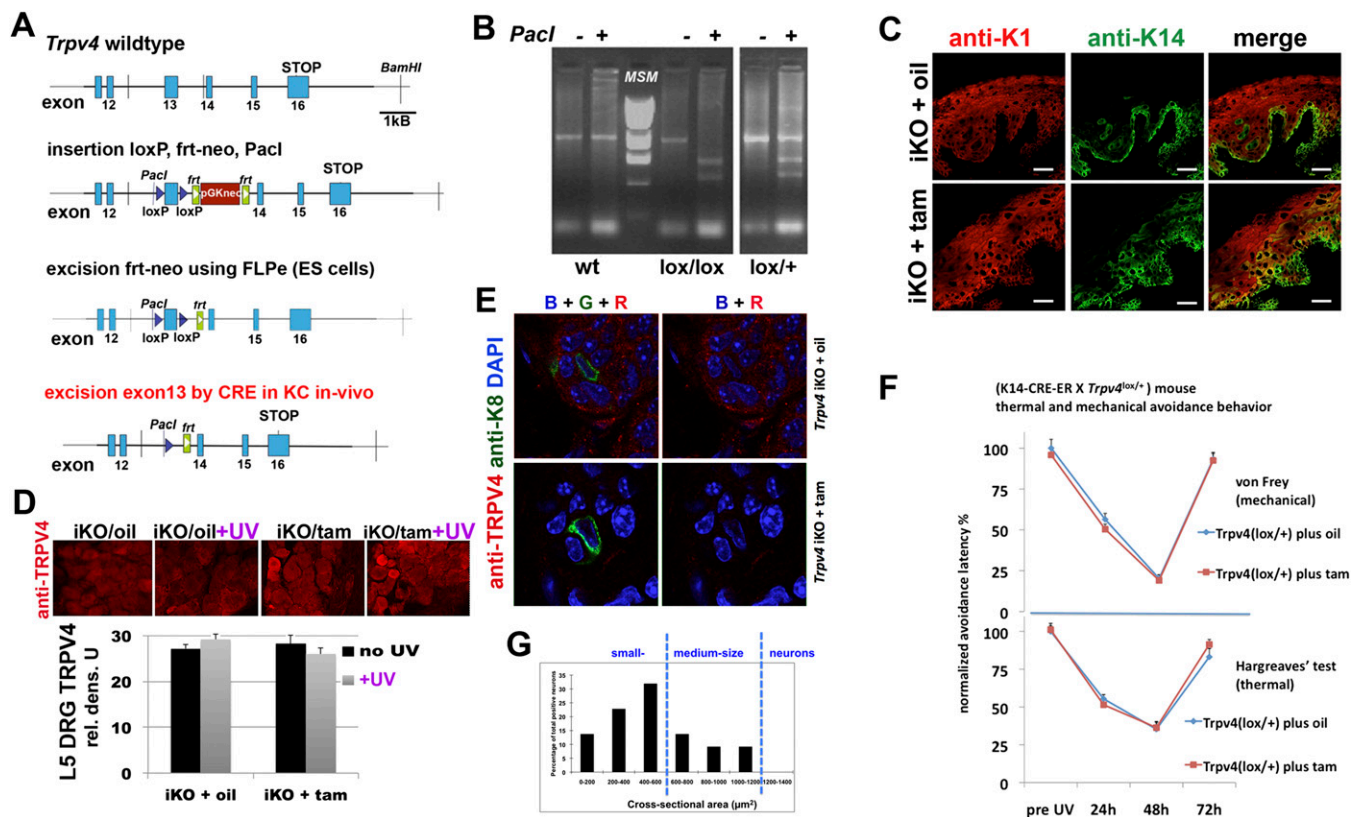


Fig. S1. Keratinocyte-specific and inducible *Trpv4* null mouse and its UVB response. (A) Gene targeting of *Trpv4* and genetic manipulation underlying generation of keratinocyte-specific and inducible *Trpv4* knockout mice. Shown are sequential steps of mouse *Trpv4* targeting, starting with flanking *Trpv4* exon13 with loxP elements and insertion of a selection cassette, flanked by frrt sites, in mouse ES cells. After generation of chimeric mice and stable transmission of the engineered mutation, the selection cassette was removed by FLPase in mice. Resulting mice were homozygosed and crossed with K14-CRE-ER^{tam} mice (1), which then permitted keratinocyte-specific and inducible *Trpv4* knockout/knockdown. (B) DNA genotyping. Shown are PCR products of WT, heterozygote, and homozygous *Trpv4*^{lox/lox} mice. Note that the PCR products needed to be digested with Pacl, and that all mice were prescreened to be CRE+ by another genotyping PCR. (C) Colabeling of mouse skin for keratin-1 (K1) and keratin-14 (K14) indicate the established pattern for vehicle-induced control mice (Upper) and a similar pattern for specific TRPV4 knockdown in keratinocytes (Lower). However, in these animals note a slightly increased expression of K14 in the stratum spinosum, reflecting attenuated TRPV4 expression and thus reduced Ca²⁺ influx. K14 is normally down-regulated at the basal-to-suprabasal transition, concomitant with the rise in Ca²⁺ signaling and induction of terminal differentiation. (D) TRPV4 protein expression in L5 DRG neurons is not different between genotypes. Densitometry of TRPV4 immunohistochemistry in L5 (foot-pad innervating) DRG neurons (upper micrographs); the bar diagram illustrates the lack of a difference in terms of TRPV4 protein abundance in oil- vs. tamoxifen-treated mice, for both baseline and 48 h after UV exposure, confirming the specificity of TRPV4 knockdown in skin when using K14 as CRE driver. Note the characteristic morphology of decorated cells identifying them as DRG sensory neurons. Note also the different levels of TRPV4 expression in these neurons, as noted previously (2–4); *n* = 3 mice per group, ≥50 neurons per mouse. (E) Lack of TRPV4 expression in Merkel cells in foot-pad epidermis. A confocal triple-fluorescent micrograph panel is shown, depicting representative images of immuno-labeled paw pads from inducible *Trpv4* knockout (iKO) control vs. tamoxifen-induced mice. Note complete knockdown of TRPV4 in this example (red channel). For Merkel cells (green channel), an anti-cytokeratin 8 antibody was used. Note lack of TRPV4 colabeling in Merkel cells. Blue channel, DAPI. (F) Lack of effect of tamoxifen application in K14-CRE-ER^{tam} mice on UVB behavioral sensitization. Note very similar withdrawal thresholds in K14-CRE-ER^{tam} X *Trpv4*^{lox/+} mice (*Trpv4* heterozygotes in keratinocytes when induced with tamoxifen) for noxious mechanical (Upper) and thermal (Lower) stimulation; *n* = 7 mice per group. Also note the time course with peak sensitivity at time point 48 h. (G) Size distribution of pERK-expressing L5 DRG neurons in oil-treated iKO mice, exposed to UVB. The bar diagram illustrates size prevalence of small and medium-size sensory neurons that express pERK 48 h after UVB exposure; note the absence of larger neurons (>1,200 µm²), *n* = 22 neurons.

- Vasioukhin V, Degenstein L, Wise B, Fuchs E (1999) The magical touch: Genome targeting in epidermal stem cells induced by tamoxifen application to mouse skin. *Proc Natl Acad Sci USA* 96(15):8551–8556.
- Liedtke W, Friedman JM (2003) Abnormal osmotic regulation in *trpv4*^{-/-} mice. *Proc Natl Acad Sci USA* 100(23):13698–13703.
- Grant AD, et al. (2007) Protease-activated receptor 2 sensitizes the transient receptor potential vanilloid 4 ion channel to cause mechanical hyperalgesia in mice. *J Physiol* 578(Pt 3): 715–733.
- Chen Y, et al. (2013) Temporomandibular joint pain: A critical role for *Trpv4* in the trigeminal ganglion. *Pain* 154(8):1295–1304.

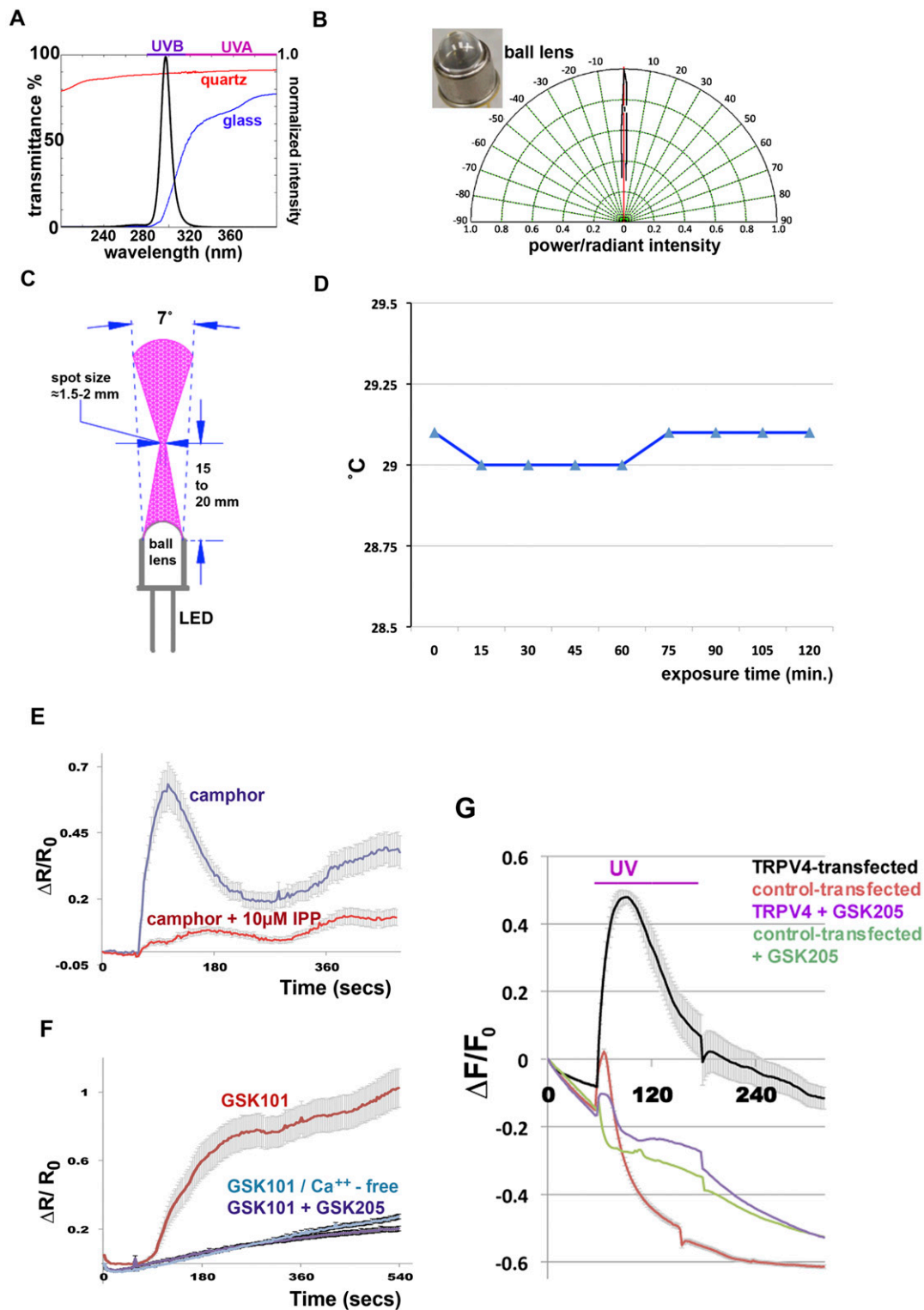


Fig. S3. UVB stimulation device and UVB keratinocyte control experiments. (A) UV spectrum emitted by the LEDs, overlapped with the spectrum of quartz (red trace), which is almost fully permeable to UVB, and glass (blue trace), which has a very low UVB permeability. The UV LED emission spectrum is plotted in black, and the transmittance spectra of the glass and quartz coverslip are in blue and red, respectively. The result showed the transparent window of the quartz coverslip correlated well with the entire UV emission wavelength of the light source, whereas the glass coverslip had only 10% transparency at the peak emission wavelength. The integrated UV light passing through the quartz coverslip was 88.9% but only 13.7% for the glass coverslip. (B) Focusing properties of the ball lens. (C) Focal geometry of the combination of UV LED and ball lens. (D) Absence of thermal effects of the UV LEDs; measurement of temperature in the focal point over time. The thermal probe was immersed in a tissue culture device as used for Fig. 4, containing Ca²⁺ imaging buffer. (E) TRPV3 activation experiment. Induction of a Ca²⁺ transient by camphor, which can be blocked effectively by 10 μM IPP, suggesting TRPV3-mediated signaling. See Fig. 4G for lack of effect of 10 μM IPP on the UVB-Ca²⁺ response. (F) TRPV4 selective activator GSK101-related findings. Ca²⁺ transient in 1^oMK in response to 5 nM GSK101, which can be completely blocked by 20 μM GSK205, suggesting it is specifically mediated by TRPV4. The GSK101-response can also be eliminated by Legend continued on following page

